

Structural Determinants for High-Affinity Binding in a Nedd4 WW3* Domain-Comm PY Motif Complex

Voula Kanelis,¹ M. Christine Bruce,^{2,3}
Nikolai R. Skrynnikov,^{3,4,5} Daniela Rotin,^{1,2,3,*}
and Julie D. Forman-Kay^{1,3,*}

¹ Programme in Structural Biology and Biochemistry

² Programme in Cell Biology

Hospital for Sick Children

Toronto, Ontario M5G 1X8

Canada

³ Department of Biochemistry

⁴ Department of Medical Genetics

University of Toronto

Toronto, Ontario M5S 1A8

Canada

Summary

Interactions between the WW domains of *Drosophila* Nedd4 (dNedd4) and Commissureless (Comm) PY motifs promote axon crossing at the CNS midline and muscle synaptogenesis. Here we report the solution structure of the dNedd4 WW3* domain complexed to the second PY motif (²²⁷TGLPSYDEALH²³⁷) of Comm. Unexpectedly, there are interactions between WW3* and ligand residues both N- and C-terminal to the PY motif. Residues Y232'–L236' form a helical turn, following the PPII helical PY motif. Mutagenesis and binding studies confirm the importance of these extensive contacts, not simultaneously observed in other WW domain complexes, and identify a variable loop in WW3* responsible for its high-affinity interaction. These studies expand our general understanding of the molecular determinants involved in WW domain-ligand recognition. In addition, they provide insights into the specific regulation of dNedd4-mediated ubiquitination of Comm and subsequent internalization of Comm or the Comm/Roundabout complex, critical for CNS and muscle development.

Introduction

The WW domains of neuronal precursor cell expressed developmentally downregulated 4 (Nedd4) (Kumar et al., 1992), a ubiquitin ligase, are small protein-protein interaction modules containing two highly conserved tryptophans and an invariant proline (Bork and Sudol, 1994). WW domains bind proline-containing regions of varying sequences in their target molecules, and have been previously classified based on these recognition sequences (Macias et al., 2002). Group I WW domains bind the PY motif (L/PPxY) (Chen and Sudol, 1995; Kasanov et al., 2001), group II domains bind the PxxP sequence (Bedford et al., 1997), group III domains interact with regions rich in Pro and Arg (Bedford et al., 2000) or

containing Pro, Met, and Gly (Bedford et al., 1998), and group IV domains bind phosphoSer- or phosphoThr-Pro (pS/T-P) sequences (Lu et al., 1999; Verdecia et al., 2000). In some cases, a specific WW domain can bind more than one type of ligand, albeit with varying affinities (Kato et al., 2004; Wiesner et al., 2002). Thus, classification of WW domains by their target ligands does not provide a complete picture of the molecular basis of recognition for these domains. The few previously solved structures of WW domain complexes (Huang et al., 2000; Kanelis et al., 2001; Pires et al., 2001, 2005; Toepert et al., 2003; Verdecia et al., 2000) indicate that core binding residues in the ligands, regardless of type, adopt a PPII helical conformation and contact homologous residues in the WW domain. Additional binding energy and specificity is provided by contacts outside these core regions, as seen most notably in the rNedd4 WW4-βENaC complex (Kanelis et al., 2001) (Nedd4 WW numbering, as in Henry et al. [2003]) and the dystrophin-β-dystroglycan complex (Huang et al., 2000), adding another layer of complexity to recognition of specific sequences by individual WW domains. Interactions outside the core binding motif are essential for determining specificity and enhancing affinity.

Members of the Nedd4 family of ubiquitin ligases, which target membrane proteins for endocytosis (Rotin et al., 2000), have a common modular architecture comprised of an N-terminal C2 domain, two to four tandem WW domains, and a C-terminal catalytic Hect domain. The Nedd4 WW domains have been shown to interact with PY motif sequences in their substrate molecules, leading to ubiquitination of the target protein. While this common architecture and core WW domain binding specificity suggest redundant cellular roles for Nedd4 proteins, specific cellular functions have been ascribed to family members (reviewed in Ingham et al., 2004; Rotin et al., 2000). For example, Nedd4-2 (and human Nedd4-1) are involved in downregulation of the epithelial sodium channel (ENaC) (Abriel et al., 1999; Kamynina et al., 2001; Snyder et al., 2001; Staub et al., 1996), a channel that harbors PY motifs (Schild et al., 1996), which are deleted or mutated in Liddle's syndrome, a hereditary form of hypertension (Lifton et al., 2001). Binding of ENaC PY motifs by the third and fourth WW domains of Nedd4-2 is necessary for channel downregulation (Kamynina et al., 2001). Specifically, the presence of a high-affinity binding WW domain, WW3*, in Nedd4-2 and some Nedd4-1 proteins is essential for this process (Henry et al., 2003), as Nedd4 proteins lacking WW3* weakly suppress channel activity. The ability to preferentially bind distinct PY motif ligands with differing affinities is one mechanism that underlies the different Nedd4 cellular specificities. Although there are several structures of WW domains, there are only a few structures of WW domain-ligand complexes, and none of the high-affinity WW3* domain. Therefore, additional structural studies are required to probe the mechanisms of sequence-specific recognition and, in particular, to understand how WW domain interactions contribute to the biological specificity of Nedd4.

*Correspondence: drotin@sickkids.ca (D.R.); forman@sickkids.ca (J.D.F.-K.)

⁵ Present address: Department of Chemistry, Purdue University, West Lafayette, Indiana 47907.

Commissureless (Comm) is a target for *Drosophila* Nedd4 (dNedd4), where dNedd4 contains three WW domains (WW1, WW3*, and WW4) (Henry et al., 2003). Comm is a single-pass transmembrane protein (Tear et al., 1996) with two PY motifs (²¹⁸ESPPCYTIATGLPSY DEALH²³⁷, PY motifs in bold) spaced closely together in its cytoplasmic C terminus. Binding of dNedd4 WW domains to these PY motifs results in ubiquitination of Comm and subsequent internalization and sorting of the Comm/Roundabout (Robo) complex, promoting axon crossing at the CNS midline (Myat et al., 2002). Comm internalization is also important in the muscle. We have recently demonstrated that binding of dNedd4 to Comm, and its subsequent ubiquitination, is responsible for removal of Comm from the muscle cell surface (Ing et al., submitted), a necessary step for motoneuron innervation (Wolf et al., 1998).

Here we report the solution structure of the high-affinity dNedd4 WW3* domain bound to the second PY motif in Comm, ²²⁷TGLPSYDEALH²³⁷, herein referred to as the LPSY peptide. Interestingly, interactions with the WW3* domain are observed for residues both N- and C-terminal to the PY motif, comprising residues T227'-L236' of Comm. (Comm residues are denoted by a prime symbol, to distinguish them from dNedd4 WW3* domain residues.) Binding experiments with mutant peptides confirm the importance of the extensive interactions observed in the dNedd4-Comm complex. Furthermore, mutation of the β 1/ β 2 loop in dNedd4 WW4 to conserved residues present in WW3* domains confers high-affinity binding to LPxY and PPxY peptides. These results highlight the importance of interactions outside the core binding region in WW domain-ligand recognition, and emphasize their importance in imparting specificity to ubiquitin-mediated regulation of Comm in developmental processes.

Results

Solution Structure of dNedd4 WW3* Domain-Comm LPSY Peptide Complex

Preliminary experiments in our laboratory indicated that the affinity of the dNedd4 WW3* domain for the Comm PY motifs is high in comparison with other WW domain-PY motif complexes (P. Henry and D. Rotin, unpublished data). In addition, our previous work showed that WW3* domains from hNedd4-1 and h/x/mNedd4-2 bound ENaC PY motifs with higher affinity than other Nedd4 WW domains (Henry et al., 2003). In order to determine the molecular basis for this high-affinity binding, we have solved the solution structure of a complex between the dNedd4 WW3* domain and a peptide derived from the LPSY region of Comm.

An overlay of the 30 lowest energy structures is shown in Figure 1A, with structural statistics in Table 1. With the exception of a few residues at the N- and C termini, both the dNedd4 WW domain and Comm LPSY peptide are well defined, having a backbone rmsd of 0.48 ± 0.10 Å for residues L531-R561 in the WW domain and T227'-L236' in the LPSY peptide. The dNedd4 WW3* domain structure is very similar to previously solved WW domain structures, including the rNedd4 WW4 domain in complex with the β ENaC PY motif-containing peptide previ-

ously solved in our laboratory (Kanelis et al., 2001). The WW domain structure consists of a three-stranded anti-parallel β sheet (Figure 1B) that is stabilized by a hydrophobic cluster formed in part by the first conserved tryptophan (W535) and the invariant proline (P560). The peptide binding site is formed by hydrophobic and uncharged groups of residues located throughout the domain (Figures 1B and 2). Specifically, residues in the β 1 (Q538), β 2 (F546, I548), and β 3 (T555) strands, in the β 1/ β 2 (A540, P541, N542), β 2/ β 3 (the uncharged H550 and the aliphatic portion of R553), and in the C-terminal loops (W557) bind the LPSY peptide (Figures 1B and 2A).

The bound peptide can be divided into three interacting regions, the LPSY core, C-terminal and N-terminal regions. The LPSY sequence of the ligand binds the WW domain as seen in other WW domain-PY motif complexes. Residues L229'-S231' adopt a PPII helical conformation, seen for PPxY ligands bound to WW domains (Huang et al., 2000; Kanelis et al., 2001; Pires et al., 2001). L229' and P230' are involved in stacking interactions with the second conserved tryptophan, W557, and F546 of the XP groove. This type of interaction is generally seen in complexes of WW domains, SH3 domains, EVH1 domains and profilin (Zarrinpar and Lim, 2000). As for other WW domain-PY motif complexes (Huang et al., 2000; Kanelis et al., 2001; Pires et al., 2001), the Comm LPSY peptide binds the dNedd4 WW3* domain in the negative orientation, in which the invariant Pro stacks against the conserved F546 rather than the binding site Trp as seen for ligands in the positive orientation (Verdecia et al., 2000). The conserved PY motif tyrosine, Y232', interacts with I548, H550, and the aliphatic portion of R553, adopting an orientation seen in the other WW domain-peptide complexes. In addition to interactions of the T555 methyl group with PY motif and C-terminal residues (see below), the hydroxyl is oriented toward the carbonyl of P230' in a potential hydrogen bond. This intermolecular hydrogen bond is also observed in the Pin1-CTD and the YAP65 WW domain-PY motif complexes (Pires et al., 2001; Verdecia et al., 2000). Of note, most WW domains (Schultz et al., 1998), including those from Nedd4 proteins, contain a Thr or Ser at this position, indicative of the importance of this feature to binding.

Interactions of Non-PY Motif Residues with the WW3* Domain

Surprisingly, residues both N- and C-terminal to the PY motif interact with the WW3* domain. As was observed in the rNedd4 WW4 domain- β ENaC complex (Kanelis et al., 2001), C-terminal residues adopt a helical turn conformation starting at the PY motif Tyr (since Nedd4 WW numbering is taken from Henry et al. [2003], the third WW domain in rNedd4 is defined as WW4; note that the rNedd4 WW4 domain is analogous to dNedd4 WW4, not dNedd4 WW3*). However, in the dNedd4 WW3* domain-Comm complex, this turn is extended by one residue comprising Y232'-L236', where A235' in Comm is structurally analogous to L621' in β ENaC (Figures 2 and 3B). Interactions are observed between A235' and the WW3* domain residues Q538, F546, I548, and T555. The side chain of L236' is oriented toward the binding site and interacts with I548 and H550 in dNedd4 WW3* (Figures 1B and 2A). Notably, strong NOEs are

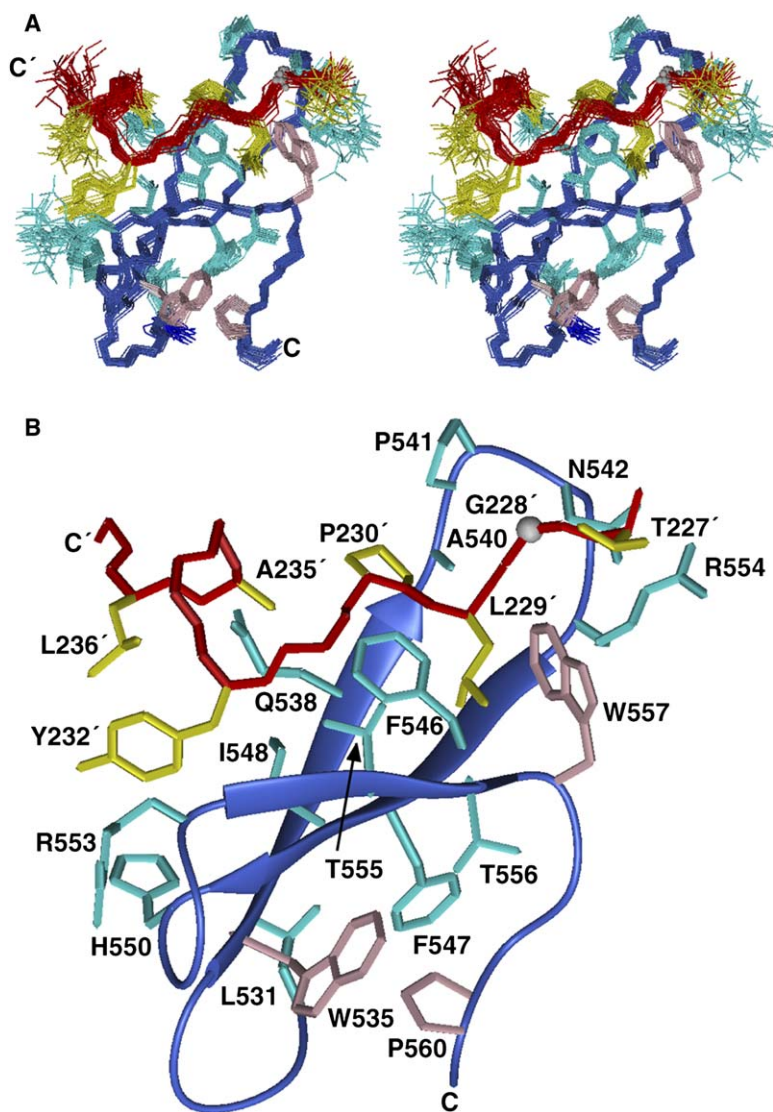


Figure 1. Solution Structure of the dNedd4 WW3*-LPSY Peptide Complex

(A) Stereo representation of a superposition of the final 30 structures.

(B) Schematic ribbon diagram of the lowest energy structure. The backbone of the WW domain is in blue. The side chains of the canonical WW domain Trp and Pro residues are shown in pink. Residues involved in packing the hydrophobic cluster and in peptide binding are shown in cyan. The LPSY peptide backbone is in red and selected side chains are shown in yellow, with the exception of Gly 228' which is shown as a gray sphere for the C α atom. Residue numbers and the C terminus for the LPSY peptide are denoted with a prime symbol (').

observed between these residues and δ -methyls of L236'. The peptide derived from β ENaC used in the structure determination of the rNedd4 complex ended at L621'. However, since the equivalent residue to Comm L236' in β ENaC is R622', it is unlikely that interactions would be formed with the analogous residues, I478 and the uncharged H480, in rNedd4. Furthermore, mutation of β ENaC R622' does not cause an increase in channel activity, in contrast to mutations of PY motif residues and L621' (Henry et al., 2003; Snyder et al., 1995).

Interactions are also seen between the β 1/ β 2 loop in the WW3* domain and residues N-terminal to the LPSY sequence. In contrast, analogous interactions were not observed in the rNedd4 WW4 domain- β ENaC complex (Figures 2 and 3A), even though the peptide used in that structure determination contained eight β ENaC residues N-terminal to the PY motif. In addition to A540, which forms the back of the XP groove, P541 and N542 in the dNedd4 WW3* domain bind residues T227'-P230' in the LPSY peptide. Although the side chain of T227' in the ensemble of structures is not as well defined as those of the PY motif residues in the li-

gand, NOEs are observed between the side chains of T227' and W557. The side chain of R554 in the β 1/ β 2 loop is oriented toward T227', and may provide additional interactions. However, due to spectral overlap, NOEs between R554 and T227' could not be unambiguously assigned. The side chains of A540, N542, R554, and W557 form a groove in which the backbone of T227' and G228' bind (Figure 2A). These structural features support the evidence from binding data (see below) that the N terminus makes important contributions to the dNedd4 WW3* domain-Comm LPSY interaction.

The dNedd4 WW3* domain-Comm LPSY structure is the only reported case of a WW domain complex in which ligand residues both N- and C-terminal to the PY motif bind the WW domain. This comprises a more extensive interaction surface than that seen for other isolated WW domain-peptide complexes that employ only the PY motif for binding (Pires et al., 2001). A surface area of $895 \pm 40 \text{ \AA}^2$ is buried upon complex formation in the dNedd4 WW3* complex, compared with $\sim 620\text{--}730 \text{ \AA}^2$ in other complexes.

Table 1. Structural Statistics for the 30 Final Structures of the dNedd4 WW3* Domain-Comm LPSY Peptide Complex

Rmsds from distance restraints (Å)		
All (2370)	0.009 ± 0.002	
Unambiguous (1741)	0.010 ± 0.002	
Ambiguous (697)	0.009 ± 0.004	
Rmsds from dihedral angle restraints (°)		
Deviations from idealized geometry		
Bonds (Å)	0.002 ± 0.00007	
Angles (°)	0.314 ± 0.009	
Impropers (°)	0.174 ± 0.011	
PROCHECK (Laskowski et al., 1996)		
Ramachandran map analysis		
Most favored regions	65.7% ± 6.5%	
Additional allowed regions	30.2% ± 6.4%	
Generously allowed regions	3.4% ± 2.1%	
Disallowed regions	0.7% ± 1.3%	
Atomic Rmsd (Å) from Mean Structure		
	Backbone	All Heavy Atoms
WW3 (531–561), LPSY (227'–236')	0.48 ± 0.10	0.81 ± 0.16
WW3 (531–561), LPSY (227'–236')	0.31 ± 0.09	0.69 ± 0.15
WW3 (531–561), LPSY (227'–236')	0.62 ± 0.23	0.96 ± 0.26

Contributions of LPSY Peptide Residues to Binding Affinity

The affinity of the dNedd4 WW3* domain for the LPSY peptide is higher than observed for other WW domain-PY motif complexes, having a K_d value of $\sim 3 \mu\text{M}$ (Table 2). We used a mutagenesis approach to further investigate the role of interactions in the high-affinity dNedd4 WW3* domain-Comm LPSY complex.

Previous experiments have indicated that the invariant Pro and Tyr residues of the PY motif contribute essential interactions. The Comm ligand has a Leu in place of the more canonical Pro in the first position of the PY motif. Many intermolecular NOEs are observed between the L229' aliphatic side chain, particularly the methyls, and A540, F546, T555, and W557 in the WW3* domain. Of note, one of the methyls of this Leu has an upfield chemical shift of -0.91 ppm, due to its location in this ar-

omatic pocket. Mutation of L229' to Pro, thereby creating a canonical PY motif, results in a ~ 2 -fold reduction in binding affinity. Having a Leu instead of a Pro is expected to decrease the amount of PPII helix of the unbound LPSY peptide, and hence its affinity for the WW domain. However, the greater enthalpic contributions from the larger Leu residue compensate for the loss of PPII helical conformation. Studies of SH3 domain binding indicate that other hydrophobic residues, such as Leu and Val, are tolerated at this position, and in some cases are preferred, since they can achieve as good or better packing than a Pro (Lim et al., 1994; Yu et al., 1994).

We investigated the contributions of the C-terminal L236' and H237' to binding. The H237'A mutation had little effect on binding affinity, in agreement with our solution structure, in which H237' makes limited interactions with the dNedd4 WW3* domain. Mutation of L236' resulted in a 2- to 3-fold decrease in binding. Although interactions are observed between I548 and H540 in the WW domain and the δ -methyls of L236', the Ala mutant likely makes similar contacts, thus partly compensating for removal of L236'. Residues D233' and E234' were not altered. These residues do not interact with the WW3* domain. Therefore, mutation of these residues likely would not alter binding, as was demonstrated for the analogous βENaC residues, D619' and S620', which adopt a similar bound conformation and do not interact with the rNedd4 WW4 domain (Henry et al., 2003; Kanelis et al., 2001). Mutation of the N-terminal T227' results in a 4-fold decrease in binding, indicating the importance of N-terminal interactions to the dNedd4 WW3* domain-Comm LPSY association. From our structure, interactions are formed between the methyl of Thr 227' to W557. Since the backbone of residues T227'–G228' is nestled in the groove that extends from the XP pocket, it is unlikely that conformational changes in the peptide occur in order to promote analogous interactions of the shorter Ala side chain in the mutant peptide with the WW domain. As expected, mutations of invariant PY motif residues, P230' and Y232', to Ala disrupt binding to the dNedd4 WW3* domain. In summary, mutation of any one of the interacting residues outside the core PY motif results in a moderate, yet significant, decrease in affinity. Removal of all N- and C-terminal residues in the Ac-LPSY-NH₂ peptide or their replacement by Ala

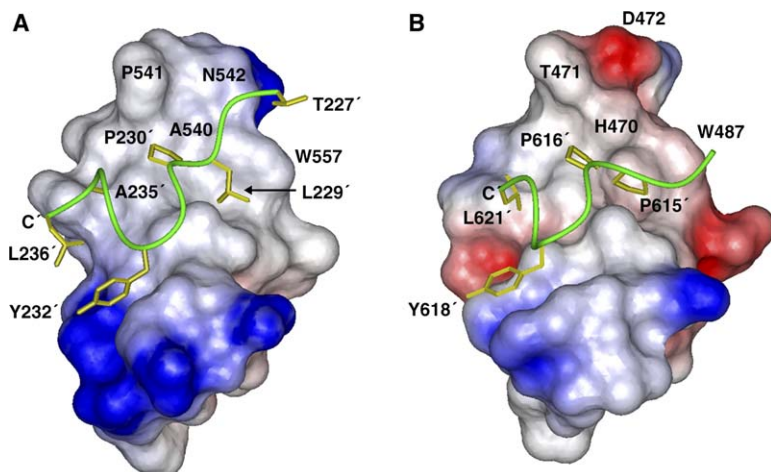


Figure 2. Comparison of the dNedd4 WW3* Domain-LPSY Peptide and rNedd4 WW4 Domain- βENaC Complexes

Molecular surfaces of the (A) dNedd4 WW3* domain and (B) rNedd4 WW4 domain (PDB code 115H) are shown with blue and red, representing positive and negative electrostatic potential, respectively. The α traces of the bound ligands are shown in green and the side chains of residues involved in binding in yellow.

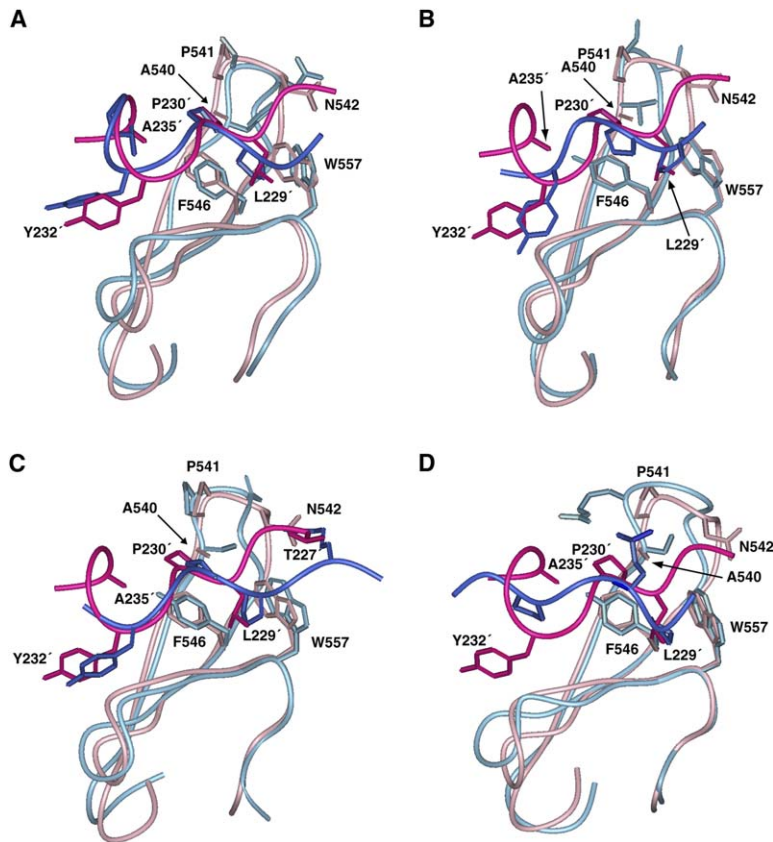


Figure 3. Comparison of WW Domain-PY Motif Complexes

The lowest energy structure from the dNedd4-Comm complex ensemble is superimposed with (A) rNedd4 WW4 domain-βENaC (PDB code 115H), (B) YAP65 WW domain-GTTPPPYTVG (PDB code 1JM0), (C) dystrophin-β-dystroglycan (PDB code 1EG4), and (D) Pin1-RNA Pol II (PDB code 1F8A) complexes. The backbone and side chains of the dNedd4 WW3* domain are in pink, while those of the LPSY peptide are in red. The backbone and side chains of the comparative WW domain are in light blue, while those of the bound ligands are in dark blue. In each case, residues L531-R561 in the dNedd4 WW3* domain were superimposed with the corresponding residues in the other WW domains. In addition, ligand residues common to both complexes were included in the superposition. The orientations between (A), (B), (C), and (D) are slightly different in order to visualize differences. FIGURES 1-3 were generated using MOLMOL (Koradi et al., 1996).

decreases binding by ~50- to 100-fold, illustrating the importance of specific residues outside the PY motif core to the high-affinity dNedd4 WW3* domain-Comm LPSY interaction.

Binding experiments performed between a peptide with two additional residues on each of the N and C termini, ²²⁵IATGLPSYDEALHHQ²³⁹, and the WW3* domain gave K_d values identical to that of the shorter peptide, indicating that we have not missed key interactions by truncating the peptide. We also tested binding of the dNedd4 WW3* domain to a peptide derived from the first PY motif in Comm, ²¹⁸ESPPCYTIAT²²⁷. Surprisingly, binding was not observed between the dNedd4 WW3* domain and this peptide, even though it has a canonical

PY motif. Binding experiments done previously in higher ionic strength (150 mM NaCl versus 20 mM used here) also showed no binding (P. Henry and D. Rotin, unpublished data).

Contributions of dNedd4 WW3* Domain Residues to Binding Affinity

To further probe the interactions responsible for high-affinity binding, mutations were made in the dNedd4 WW3* domain, and binding to the LPSY peptide was measured. Previous experiments had been done to examine the role of WW domain residues to binding of the core PY motif. Mutation of the binding site Trp to Ala abrogates binding (Chen et al., 1997) due to obliteration of

Table 2. Dissociation Constants for dNedd4 WW Domain-Comm Peptide Interactions

Peptide Sequence ^a	WW3*	WW4	H591A/T592P/D593N WW4
²²⁷ TGLPSYDEALH ²³⁶	3.1 ± 0.5 (3)	NB	2.9 ± 0.8 (2)
<u>A</u> GLPSYDEALH	12.0 ± 3.3 (4)		
TG <u>P</u> PSYDEALH	6.7 ± 0.9 (4)	22.2 ± 2.3 (2)	5.9 ± 1.0 (3)
TGLPSYDEAA <u>H</u>	8.0 ± 3.5 (3)		
TGLPSYDEAL <u>A</u>	4.1 ± 0.4 (3)		
TG <u>A</u> PSYDEALH	NB		
TGLPS <u>A</u> DEALH	NB		
²²⁵ IATGLPSYDEALHHQ ²³⁸	3.2 ± 0.7 (3)		
²¹⁸ ESPPCYTIAT ²²⁷	NB		
Ac-LPSY-NH ₂	158.8 ± 34.8 (3)		
<u>A</u> ALPSYAAAA	210.5 ± 48.2 (4)		

The equilibrium dissociation constants (K_d , μ M) were determined using intrinsic tryptophan fluorescence and are reported as averages ± standard deviations. The number in parentheses indicates number of experiments performed for each binding analysis. NB, no observable binding.
^a Underlined residues denote mutations.

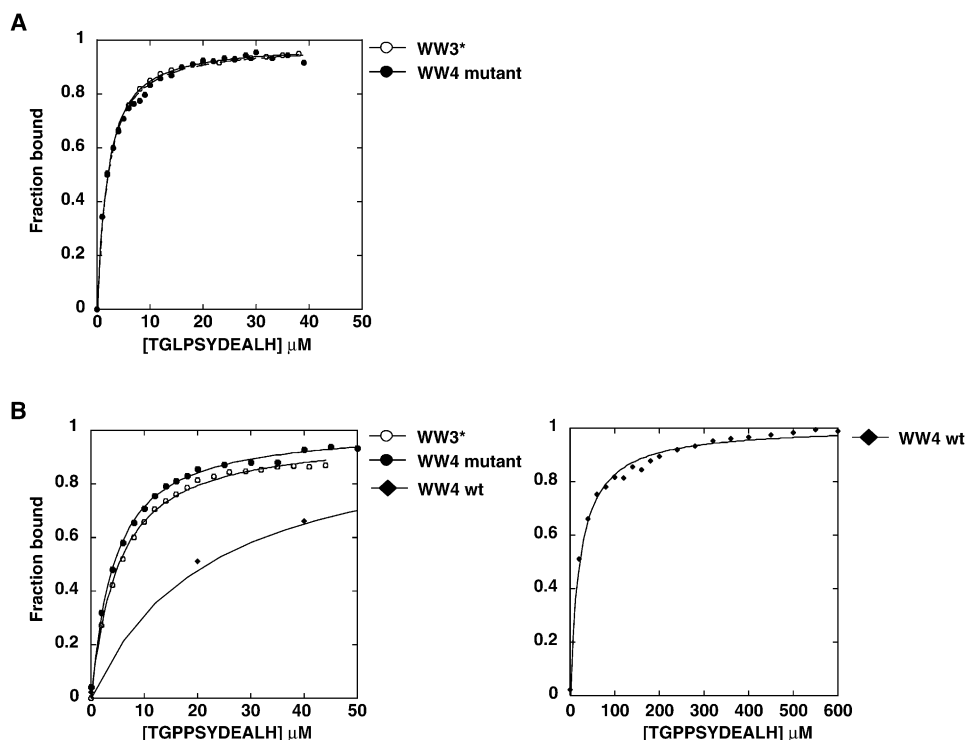


Figure 4. Binding of the dNedd4 WW Domains to LPSY Peptide as Monitored by Intrinsic Tryptophan Fluorescence

Binding of the Comm (A) wild-type LPSY and (B) mutant L229'P peptides is shown to the dNedd4 WW3* and dNedd4 WW4 wild-type and $\beta 1/\beta 2$ loop mutant domains. For comparison, the first few points of the WW4 wild-type-L229'P titration is displayed on the plot for the WW3* and WW4 mutant-L229'P titrations, with the full WW4 wild-type-L229'P data set displayed to the right.

the XP groove. Changing the aliphatic residue in the Tyr binding pocket (Ile 548 in dNedd4) of the YAP65 WW domain to an aromatic changes its specificity from PY motifs to PxxP ligands (Espanel and Sudol, 1999; Kato et al., 2004), and increasing the number of Arg and Lys residues results in recognition of a PY motif with a phosphorylated Tyr (Toepert et al., 2003). However, little has been done to investigate contributions of WW domain residues that bind sequences outside the core PY motif. Our focus in this study was the contribution of the $\beta 1/\beta 2$ loop, due to its importance in binding the LPSY peptide.

The dNedd4 WW3* domain complex structure illustrated the involvement of the $\beta 1/\beta 2$ loop residues, P541 and N542, in binding the LPSY peptide. The corresponding residues in the rNedd4 WW4 domain (T471 and D472), which are conserved in dNedd4 WW4, are not involved in βENaC binding. This result, along with the observation that the sequence APN is conserved in the $\beta 1/\beta 2$ loop of all high-affinity binding Nedd4 WW3* domains, highlighted this sequence as being necessary for a strong interaction with ligand. To test this hypothesis, we created a chimera between the dNedd4 WW3* and WW4 domains by replacing the sequence HTD in WW4 with APN. The wild-type and mutant WW4 domains were tested for binding to the wild-type LPSY peptide and L229'P mutant, which has a canonical PY motif, and compared to that seen for the WW3* domain (Figure 4). The K_d for the interaction between the WW4 domain mutant and the L229'P peptide is 6 μM —a ~ 3 - to 4-fold increase in affinity over the wild-type WW4 domain and identical to the WW3* domain (Figure 4B). This

gain of function is also observed for binding of the wild-type LPSY peptide to the WW4 domain mutant, which has a K_d value of $\sim 3 \mu\text{M}$, identical to what is observed for binding to the WW3* domain (Figure 4A). Previously, we observed that mutations of A540 and P541 residues in WW3* to the corresponding His and Thr in WW4 decreased binding by ~ 4 -fold, but that the reverse mutations did not restore high-affinity binding of the Nedd4 WW4 domain (Henry et al., 2003). Therefore the sequence of all three residues of the $\beta 1/\beta 2$ loop, A540, P541, and N542, is the necessary and sufficient determinant in Nedd4 WW3* domains for high-affinity binding.

Surprisingly, the wild-type dNedd4 WW4 domain binds the wild-type LPSY peptide very weakly, as saturation was not achieved even at peptide concentrations of 0.5 mM for 1 μM protein. The WW4 domain does bind the L229'P mutant, with a K_d value of $\sim 22 \mu\text{M}$, which is similar to what we observed for the rNedd4 WW4 domain binding to βENaC (PPNYDSL) (Kanelis et al., 2001), indicating that the isolated dNedd4 WW4 domain is properly folded. We predict that the discrimination for the smaller Pro instead of the Leu in the variable binding position of the XP groove is due to the bulky His in the $\beta 1/\beta 2$ loop of the WW4 domain. This residue forms the back of the XP groove and results in structural differences in ligand side chains in the binding site (Macias et al., 2002, and see below).

Discussion

Our solution structure of the dNedd4 WW3* domain-Comm LPSY peptide complex and binding experiments

provide evidence for the importance of residues outside the core L/PPxY binding motif for affinity and specificity in WW domain interactions. This is the only WW domain-ligand complex solved to date where peptide residues both N- and C-terminal to the core PY motif contact the domain.

Comparison with the rNedd4 WW4 Domain-βENaC Complex

Although the structures of the dNedd4 WW3* domain-Comm LPSY and rNedd4 WW4-βENaC PPNY complexes are similar, observed differences provide structural insights into the mechanism of high-affinity binding of WW3* domains (Figure 3A and Figure S1 in the Supplemental Data). Of note, the sequence identity between the WW4 domains from rNedd4 and dNedd4 is 81%, with all binding site residues identical (Henry et al., 2003). Therefore, structural differences observed between the dNedd4 WW3*-Comm LPSY and rNedd4 WW4-βENaC complexes are not due to a difference in species, but rather the WW domains (therefore, these WW domains are referred to as WW3* and WW4, respectively). The bulky His in WW4 sterically inhibits binding of L229', while the smaller Ala in WW3* creates a groove that accommodates the LPSY peptide. Furthermore, P541 and N542 in the β1/β2 loop of WW3* provide favorable groups for binding the hydrophobic LPSY peptide compared with a Thr and negatively charged Asp, respectively, in WW4. In the rNedd4 WW domain, the side chains of T471 and D472 are oriented away from the binding site and do not contact βENaC. Due to the N-alkyl substitution of proline residues, P541 in dNedd4 WW3* is restricted in its conformation and is not able to adopt orientations seen for the side chain of T471 in rNedd4 WW4. Therefore, in addition to providing increased interactions with ligand, P541 may also restrict the conformations of the β1/β2 loop in the free WW3* domain, resulting in a smaller entropic cost upon binding, which ultimately leads to a higher affinity interaction. The combination of the smaller Ala and favorable residues in the β1/β2 loop for ligand binding results in a displacement of residues N542–T545 toward the N terminus of the ligand in the WW3* domain complex relative to the WW4 domain complex. Therefore, as seen for SH3 domains, variable loops in WW domains are necessary to achieve specificity and enhance affinity. While residues in the β2/β3 loop are involved in ligand binding in all WW domain-PY motif complexes, the involvement of the β1/β2 loop is not always observed. Not only is the β1/β2 loop involved in binding N-terminal residues in the LPSY peptide, the naturally occurring APN sequence imparts high-affinity binding to Nedd4 WW3* domains.

There are also differences in side chain orientations of XP groove binding residues between the two complexes. The invariant Pro residues in Comm (P230') and βENaC (P616') make stacking interactions with a Phe in their respective WW domains. However, due to the bulky His at the back of the XP groove in WW4, the backbone of P615' and P616' in βENaC is shifted away from the WW domain compared with that of L229' and P230' in the WW3* domain-LPSY complex. This difference in conformation propagates so that the side chain of P615' in βENaC is buried deeper between the Phe and

Trp aromatic rings in WW4 than the corresponding Comm L229' bound to WW3*. The larger Leu in the LPSY peptide can not be accommodated in the XP groove of the WW4 domain in the orientation adopted by P615' in βENaC, explaining the observation that the dNedd4 WW4 domain doesn't bind the LPSY peptide (Table 1). A comparison of the two complexes also reveals a displacement of the backbone of the C-terminal helical turn of the bound ligand, so that the methyl groups of A235' in the LPSY peptide and L621' in βENaC are in identical positions and make conserved interactions with the respective WW domain. This flexibility implies that other methyl-containing residues could be accommodated C-terminal to the PY motif, and suggests the possibility that this is a conserved interaction in Nedd4 WW domain-ligand complexes, particularly given the sequence of Nedd4 ligands. For example, the sequence PPxYxxL is conserved in all ENaC subunits across all species, and the first PY motif of Comm also has methyl-containing residues two and three amino acids C-terminal to the Tyr. It is likely that the sequence PPxYxxϕ (where ϕ is a methyl-containing residue) is found in other Nedd4 targets.

Comparison with Other WW Domain Complexes

It is also interesting to compare the dNedd4 WW3* domain-Comm LPSY complex to other solved WW domain complexes, the dystrophin-β-dystroglycan complex (Huang et al., 2000), the YAP65 WW domain bound to LPPY and PPPY peptides (Pires et al., 2001), and the Pin1-RNA Pol II pS-P complex (Verdecia et al., 2000). Differences are observed between the dNedd4 and YAP65 complexes in the side chain positions of the PY motif residues that bind the XP groove. While L229' in Comm stacks against W557 in the dNedd4 WW3* domain, the backbone and side chains and of the corresponding Leu in the Ac-PLPPY-NH₂ peptide and Pro in the GTPPPPVTVG and N-(n-octyl)-GPPPY peptides are oriented outward from the binding site Trp in the YAP65 WW domain complexes (Figure 3B). This difference may be the reason that the YAP65 WW domain binds a canonical PY motif with higher affinity than the LPxY variant (Pires et al., 2001), opposite to what is observed for the dNedd4 WW3* domain.

Interactions with residues N-terminal to the PY motif are also present in the dystrophin-β-dystroglycan complex. These interactions are mediated by the β1/β2 loop of the WW domain and residues in the EF hand domain, which is essential, as the WW domain alone is unable to bind β-dystroglycan (Huang et al., 2000). Although the PY motif residues in the dNedd4 and dystrophin complexes can be superimposed quite well, the ligand N termini and β1/β2 loops are displaced between the two complexes (Figure 3C). This is caused by different side chain orientations of T227' in Comm compared to the residue at the equivalent position, R887, in β-dystroglycan. While the side chain of Comm T227' is oriented toward the binding site Trp in dNedd4, that of R887 in β-dystroglycan interacts with N3068 (N542 in dNedd4) in the β1/β2 loop of the dystrophin WW domain. C-terminal interactions are not observed in the dystrophin-β-dystroglycan complex, even though the peptide used in the structure determination has three residues C-terminal to the PY motif.

The importance of the $\beta 1/\beta 2$ loop in ligand binding has also been demonstrated for the group IV WW domain in Pin1, which interacts with pS/T-P-containing ligands (Verdecia et al., 2000). The ligand adopts an extended conformation in the “positive” orientation bound to the Pin1 WW domain, with RNA Pol II residues P175 and pS174 structurally analogous to L229' and P230' in Comm, respectively (Figure 3D). The analogous residue to A540 in dNedd4 is R17 in Pin1. Structural and mutagenesis data indicate that a positive charge at this position is necessary for high-affinity binding to a pS/T-P ligand (Kato et al., 2002; Verdecia et al., 2000). In addition, S16 in Pin1 in place of P541 in dNedd4 makes an additional hydrogen bond to the peptide phosphate and hence increases the affinity of the Pin1 WW domain for the pS-P peptide of RNA Pol II. Having hydrophobic residues in the $\beta 1/\beta 2$ loop of dNedd4 WW3* domain is expected to preclude its interaction with a pS/T-P ligand.

A comparison of the dNedd4 WW3* domain-Comm LPSY peptide complex with other WW domain-PY motif complexes identified structural differences in the ligand as a consequence of WW domain residues that impact affinity and specificity. These differences can occur in core residues, as well as those outside the core binding motif. Further, in contrast to group IV WW domain complexes, residues in the $\beta 1/\beta 2$ loop are not always involved in ligand binding in group I complexes. Together, these differences serve to fine-tune affinities for regulation of complex cellular processes.

Differential Binding of dNedd4 WW3* and WW4 Domains

Although the dNedd4 WW3* and WW4 domains are very similar, having a sequence identity of ~52% and 5 of 8 binding site residues identical, they have very different binding properties. Our in vitro binding experiments indicate that the affinity of the LPSY sequence in Comm for dNedd4 WW3* is much higher than for the WW4 domain. Surprisingly, the dNedd4 WW3* domain does not interact with the ESPPCYTIAT peptide, even though it is a canonical PY motif. However, our preliminary binding experiments indicate that dNedd4 WW4 interacts weakly with the ESPPCYTIAT peptide (data not shown). These results suggest a discriminatory aspect to Comm PY motif binding by the dNedd4 WW domains. WW1 is very similar in sequence to other Nedd4 WW1 domains, which we and others have shown previously to have very low affinity for PY motifs (Henry et al., 2003; Kanelis et al., 2001). The dNedd4 WW1 domain contains an Asp in place of A540 in the WW3* domain, and thus is not expected to make major contributions to binding of Comm by dNedd4. Furthermore, dNedd4 fragments pulled out in a yeast-2-hybrid screen, using the intracellular region of Comm as bait, contained only WW3* and WW4 (Myat et al., 2002). WW3* and WW4 are tandem WW domains in dNedd4. Therefore, in vivo it is likely that only WW3* binds the LPSY ligand, whereas WW4 may bind the PPCY ligand. Simultaneous binding of the Comm ligands by the dNedd4 WW3* and WW4 domains is unlikely, however, since the two PY motifs are very close to each other (218 ESPPCYTIATGLPSY DEALH 237). Methyl-containing residues are found at the C terminus of each PY motif. In a manner similar to the β ENaC PY peptide and the Comm LPSY peptide,

residues C-terminal to the PPCY sequence in Comm (Y223' to T227') likely bind the WW domain in a helical conformation. From the dNedd4 WW3*-Comm LPSY complex, we know that T227' is in an extended conformation. Thus, steric restraints between these WW domain complexes would likely preclude the simultaneous interaction of PPCY with the WW4 domain and LPSY with the WW3* domain.

Comm, in complex with Robo, is involved in regulating axon crossing of the CNS midline during *Drosophila* development (Kidd et al., 1998). This process requires sequestration of Robo away from the surface of axons (to avoid recognition by the midline repellent slit), carried out by endocytosis (Myat et al., 2002) and/or sorting (Keleman et al., 2002) of the Comm/Robo complex to endosomes. Comm LPSY-motif binding to dNedd4 plays a key role in regulating this endocytosis/sorting event. Comm endocytosis from muscle surface is also required prior to motoneuron synaptogenesis in *Drosophila* embryos (Wolf et al., 1998), a process that is mediated by dNedd4 as well (Ing et al., submitted). Since high-affinity interactions with the Comm LPSY motif require the presence of the APN sequence within the WW3* domain, and as the WW3* domain is only present in dNedd4 and not other WW-containing proteins in flies (Figure S2), dNedd4 itself, and not other family members, is involved in regulating Comm. Knocking down dNedd4 with RNAi results in the same synaptogenesis defect as the Comm PY mutant (Ing et al., submitted). Interestingly, dNedd4 is also involved in regulating endocytosis and sorting of *Drosophila* Notch, which contains a PY motif (PPSYEDCI) at its intracellular C terminus (Sakata et al., 2004; Wilkin et al., 2004). Finally, the presence of the high-affinity WW3* domain in the mammalian Nedd4-2 (and some Nedd4-1) proteins provides an explanation for the observation that only these WW3*-containing Nedd4 proteins can effectively suppress ENaC activity by regulating cell surface stability of this channel. This regulation is key to controlling salt and fluid absorption in several tissues and in the regulation of blood pressure. The work presented here illustrates the molecular basis for the high-affinity binding of Nedd4 WW3* domains to their cognate ligands and expands our understanding of the specificity of Nedd4 proteins.

Experimental Procedures

NMR Sample Preparation and NMR Spectroscopy

The second WW domain from dNedd4 (WW3*, residues 526–566) was expressed as a GST fusion at 25°C in *Escherichia coli* BL21(DE3) cells grown in minimal media with $^{15}\text{N-NH}_4\text{Cl}$ and ^{13}C -glucose as the sole nitrogen and carbon sources, respectively. The GST-WW3* protein was purified using glutathione sepharose affinity chromatography. Following digestion with PreScission protease (Amersham Biosciences), the WW domain was purified to homogeneity using a Superdex 75 column (Amersham Biosciences), as confirmed by mass spectrometry. Peptides derived from Comm were prepared synthetically using standard F-moc solid-phase chemistry and purified on a C18 reverse-phase HPLC column (Phenomenix).

NMR experiments were carried out at 15°C on a Varian Inova 500 MHz spectrometer equipped with pulse field gradients and a triple resonance probe with actively shielded z-gradients. Data were processed and analyzed using the nmrPipe/nmrDraw (Delaglio et al., 1995) and nmrView (Johnson and Blevins, 1994) software packages. Double-filtered COSY in D_2O , TOCSY, and NOESY (140 ms) spectra (Ikura and Bax, 1992) were recorded to obtain backbone and side chain assignments for the bound LPSY peptide using a sample

that contained 1.4 mM uniformly $^{15}\text{N}/^{13}\text{C}$ -labeled dNedd4 WW3* domain with 1.0 mM Comm LPSY peptide. Using equimolar amounts of the dNedd4 WW3* domain and LPSY peptide resulted in poor quality double-filtered TOCSY and NOESY spectra, likely due to broadening from exchange of bound and free LPSY peptide. Intramolecular distance restraints for the bound LPSY peptide were obtained from the double-filtered NOESY experiment.

Backbone and aliphatic side chain assignments for WW3* were obtained from standard triple resonance experiments (Kay, 1995; Sattler et al., 1999) recorded on a sample that contained equimolar amounts (1.1 mM) of $^{15}\text{N}/^{13}\text{C}$ -labeled dNedd4 WW3* domain and Comm LPSY peptide. Assignments for aromatic resonances were obtained from $(\text{H}\beta)\text{C}\beta(\text{C}\gamma\text{C}\delta)\text{H}\delta$, $(\text{H}\beta)\text{C}\beta(\text{C}\gamma\text{C}\delta\text{C}\epsilon)\text{H}\epsilon$ (Yamazaki et al., 1993), HMBC (Pelton et al., 1993), and a $^{13}\text{C}/^{15}\text{N}$ -edited NOESY-HSQC (Pascal et al., 1994) spectrum with a mixing time of 175 ms, from which intramolecular distance restraints for the dNedd4 WW3* domain were obtained. Intermolecular distance restraints were obtained from the $^{13}\text{C}/^{15}\text{N}$ -edited NOESY-HSQC spectrum and half-filtered NOESY (250 ms) (Zwahlen et al., 1997) spectrum recorded in 100% D_2O .

Structure Calculations

Preliminary structures were calculated using a torsion angle dynamics protocol within CNS 1.1 (Brunger et al., 1998). Distance restraints were assigned manually from NOESY experiments. Initially, only intramolecular dNedd4 WW3* domain NOEs having symmetry-related peaks were assigned. Only intermolecular NOEs to Comm LPSY protons with unique chemical shifts (Y232' $\text{H}\delta$, $\text{H}\epsilon$, and L229' $\text{H}\delta$), that could be unambiguously assigned, were in the first iteration. These were augmented with intermolecular NOEs obtained from the half-filtered NOESY experiment. Backbone dihedral angles for residues of the WW domain in β strands were obtained using TALOS (Cornilescu et al., 1999). Converged structures generated without violations of NOEs >0.2 Å and dihedral angle restraints $>5^\circ$ were used as input into ARIA 1.0 (Nilges and O'Donoghue, 1998) for automated assignment of all NOEs. The tolerance for automatic assignment was 0.05 ppm and 0.3 ppm in the ^1H and heteronuclear dimensions, respectively. Since stereospecific assignments were not made, a floating chirality approach was used for methylene and isopropyl groups and the $\text{H}\delta$, $\text{H}\epsilon$ protons of Phe and Tyr (Folmer et al., 1997). Seven iterations were performed, reducing the cut-off for ambiguous assignments from 0.999 to 0.80, and the violation tolerance from 0.25 Å to 0.00 Å. Thirty structures were calculated in the first six iterations, from which the best seven, as assessed by total energy, were used for the interactive NOE assignment in the next iteration. In the final iteration, 200 structures were calculated, from which the lowest 30 energy structures were used for analysis.

In addition, a second set of ARIA calculations was performed where the input structures consisted of the WW domain fold and the peptide tethered using the unambiguous intermolecular NOEs to LPSY Y232' $\text{H}\delta$, $\text{H}\epsilon$ and L229' $\text{H}\delta$ protons. The final structures from this set of calculations, where the peptide structure was not defined in the input structures, are identical to those calculated as described above (data not shown).

Binding Studies

Histidine-tagged fusion proteins of the dNedd4 WW3* (527–571) and WW4 (577–612) domains, as well as a WW4 mutant (H591A/T592P/D593N) were expressed at 25°C in *E. coli* BL21(DE3) and purified using a Ni^{2+} affinity column, followed by a Superdex 75 column. Following digestion with TEV protease, the His-tag and protease were removed using a second Ni^{2+} column. Purity and mass of the proteins was confirmed using mass spectrometry.

K_d values for dNedd4 WW domain-Comm PY motif complexes were determined using intrinsic tryptophan fluorescence. Peptide titration experiments were performed on an AVIV ATS105 fluorometer equipped with an automatic titrator, at 20°C, with excitation and emission wavelengths of 298 and 330 nm and slit widths of 2 and 4 nm, respectively. The excitation wavelength of 298 nm was chosen to avoid exciting the tyrosine residue in the peptide and the emission wavelength of 330 nm corresponds to the wavelength where fluorescence difference of free and peptide-complexed WW domains is at a maximum. Affinities were measured in 10 mM Na^+ phosphate, pH 7, 20 mM NaCl, with WW domain concentrations of 1 μM . Wild-type

and mutant peptides derived from the two PY motif-containing regions of Comm ($^{267}\text{ESPPCYTIAT}^{227}$, $^{227}\text{TGLPSYDEALH}^{237}$, and $^{225}\text{IATGLPSYDEALHHQ}^{239}$) were added at concentrations of 0 μM up to 2 mM, depending on the K_d value. Titration data were fit assuming a 1:1 complex (Viguera et al., 1994).

Supplemental Data

Supplemental data are available online at <http://www.structure.org/cgi/content/full/14/3/543/DC1/>.

Acknowledgments

We thank R. Muhandiram for assistance with NMR data collection and A. Davidson for the use of the fluorometer. Structures were calculated at the Ontario Centre for Genomic Computing. V.K. was supported by an NSERC PDF fellowship. M.C.B. is a recipient of a training fellowship (Restracom) from the Research Institute at the Hospital for Sick Children and an Ontario Graduate Scholarship. This work was supported by grants to D.R. from the Canadian Institute for Health Research and to D.R. and J.D.F.-K. from the National Cancer Institute of Canada, with funds from the Canadian Cancer Society.

Received: August 25, 2005

Revised: November 4, 2005

Accepted: November 13, 2005

Published online: March 14, 2006

References

- Abriel, H., Loffing, J., Rebhun, J.F., Pratt, J.H., Schild, L., Hori-sberger, J.D., Rotin, D., and Staub, O. (1999). Defective regulation of the epithelial Na^+ channel by Nedd4 in Liddle's syndrome. *J. Clin. Invest.* 103, 667–673.
- Bedford, M.T., Chan, D.C., and Leder, P. (1997). FBP WW domains and the Abl SH3 domain bind to a specific class of proline-rich ligands. *EMBO J.* 16, 2376–2383.
- Bedford, M.T., Reed, R., and Leder, P. (1998). WW domain-mediated interactions reveal a spliceosome-associated protein that binds a third class of proline-rich motif: the proline glycine and methio-nine-rich motif. *Proc. Natl. Acad. Sci. USA* 95, 10602–10607.
- Bedford, M.T., Sarbassova, D., Xu, J., Leder, P., and Yaffe, M.B. (2000). A novel Pro-Arg motif recognized by WW domains. *J. Biol. Chem.* 275, 10359–10369.
- Bork, P., and Sudol, M. (1994). The WW domain: a signalling site in dystrophin? *Trends Biochem. Sci.* 19, 531–533.
- Brunger, A.T., Adams, D.A., Clore, G.M., DeLano, W.L., Gros, P., Grosse-Kuntzle, R.W., Jiang, J.-S., Kuszewski, J., Nilges, M., Pannu, N.S., et al. (1998). Crystallography and NMR system: a new software suite for macromolecular structure determination. *Acta Crystallogr. D Biol. Crystallogr.* 54, 905–921.
- Chen, H.I., and Sudol, M. (1995). The WW domain of Yes-associated protein binds a proline-rich ligand that differs from the consensus established for Src homology 3-binding modules. *Proc. Natl. Acad. Sci. USA* 92, 7819–7823.
- Chen, H.I., Einbond, A., Kwak, S.J., Linn, H., Koepf, E., Peterson, S., Kelly, J.W., and Sudol, M. (1997). Characterization of the WW domain of human Yes-associated protein and its polyproline-containing ligands. *J. Biol. Chem.* 272, 17070–17077.
- Cornilescu, G., Delaglio, F., and Bax, A. (1999). Protein backbone angle restraints from searching a database for chemical shift and sequence homology. *J. Biomol. NMR* 13, 289–302.
- Delaglio, F., Grzesiek, S., Vuister, G.W., Zhu, G., Pfeifer, J., and Bax, A. (1995). NMRPipe: a multidimensional spectral processing system based on UNIX pipes. *J. Biomol. NMR* 6, 277–293.
- Espanel, X., and Sudol, M. (1999). A single point mutation in a group I WW domain shifts its specificity to that of group II WW domains. *J. Biol. Chem.* 274, 17284–17289.
- Folmer, R.H., Hilbers, C.W., Konings, R.N., and Nilges, M. (1997). Floating stereospecific assignment revisited: application to an

- 18 kDa protein and comparison with J-coupling data. *J. Biomol. NMR* 9, 245–258.
- Henry, P.C., Kanelis, V., O'Brien, M.C., Kim, B., Gautschi, I., Forman-Kay, J., Schild, L., and Rotin, D. (2003). Affinity and specificity of interactions between Nedd4 isoforms and the epithelial Na⁺ channel. *J. Biol. Chem.* 278, 20019–20028.
- Huang, X., Poy, F., Zhang, R., Joachimiak, A., Sudol, M., and Eck, M.J. (2000). Structure of a WW domain containing fragment of dystrophin in complex with beta-dystroglycan. *Nat. Struct. Biol.* 7, 634–638.
- Ikura, M., and Bax, A. (1992). Isotope-filtered 2D NMR of a protein-peptide complex: study of a skeletal muscle myosin light chain kinase fragment bound to calmodulin. *J. Am. Chem. Soc.* 114, 2433–2440.
- Ingham, R.J., Gish, G., and Pawson, T. (2004). The Nedd4 family of E3 ubiquitin ligases: functional diversity within a common modular architecture. *Oncogene* 23, 1972–1984.
- Johnson, B.A., and Blevins, R.A. (1994). NMRView: a computer program for the visualization and analysis of NMR data. *J. Biomol. NMR* 4, 603–614.
- Kamynina, E., Debonneville, C., Bens, M., Vandewalle, A., and Staub, O. (2001). A novel mouse Nedd4 protein suppresses the activity of the epithelial Na⁺ channel. *FASEB J.* 15, 204–214.
- Kanelis, V., Rotin, D., and Forman-Kay, J.D. (2001). Solution structure of a Nedd4 WW domain-ENaC peptide complex. *Nat. Struct. Biol.* 8, 407–412.
- Kasanov, J., Pirozzi, G., Uveges, A.J., and Kay, B.K. (2001). Characterizing Class I WW domains defines key specificity determinants and generates mutant domains with novel specificities. *Chem. Biol.* 8, 231–241.
- Kato, Y., Ito, M., Kawai, K., Nagata, K., and Tanokura, M. (2002). Determinants of ligand specificity in group I and IV WW domains as studied by surface plasmon resonance and model building. *J. Biol. Chem.* 277, 10173–10177.
- Kato, Y., Nagata, K., Takahashi, M., Lian, L., Herrero, J.J., Sudol, M., and Tanokura, M. (2004). Common mechanism of ligand recognition by group II/III WW domains: redefining their functional classification. *J. Biol. Chem.* 279, 31833–31841.
- Kay, L.E. (1995). Pulsed field gradient multi-dimensional NMR methods for the study of protein structure and dynamics in solution. *Prog. Biophys. Mol. Biol.* 63, 277–299.
- Keleman, K., Rajagopalan, S., Cleprien, D., Teis, D., Paiha, K., Huber, L.A., Technau, G.M., and Dickson, B.J. (2002). Comm sorts Robo to control axon guidance at the *Drosophila* midline. *Cell* 110, 415–427.
- Kidd, T., Brose, K., Mitchell, K.J., Fetter, R.D., Tessier-Lavigne, M., Goodman, C.S., and Tear, G. (1998). Roundabout controls axon crossing of the CNS midline and defines a novel subfamily of evolutionarily conserved guidance receptors. *Cell* 92, 205–215.
- Koradi, R., Billeter, M., and Wuthrich, K. (1996). MOLMOL: a program for display and analysis of macromolecular structures. *J. Mol. Graph.* 14, 51–55.
- Kumar, S., Tomooka, Y., and Noda, M. (1992). Identification of a set of genes with developmentally down-regulated expression in the mouse brain. *Biochem. Biophys. Res. Commun.* 185, 1155–1161.
- Laskowski, R.A., Rullmann, J.A., MacArthur, M.W., Kaptein, R., and Thornton, J.M. (1996). AQUA and PROCHECK-NMR: programs for checking the quality of protein structures solved by NMR. *J. Biomol. NMR* 8, 477–486.
- Lifton, R.P., Gharavi, A.G., and Geller, D.S. (2001). Molecular mechanisms of human hypertension. *Cell* 104, 545–556.
- Lim, W.A., Richards, F.M., and Fox, R.O. (1994). Structural determinants of peptide-binding orientation and of sequence specificity in SH3 domains. *Nature* 372, 375–379.
- Lu, P.J., Zhou, X.Z., Shen, M., and Lu, K.P. (1999). Function of WW domains as phosphoserine- or phosphothreonine-binding modules. *Science* 283, 1325–1328.
- Macias, M.J., Wiesner, S., and Sudol, M. (2002). WW and SH3 domains, two different scaffolds to recognize proline-rich ligands. *FEBS Lett.* 513, 30–37.
- Myat, A., Henry, P., McCabe, V., Flintoft, L., Rotin, D., and Tear, G. (2002). *Drosophila* Nedd4, a ubiquitin ligase, is recruited by Commissureless to control cell surface levels of the roundabout receptor. *Neuron* 35, 447–459.
- Nilges, M., and O'Donoghue, S.I. (1998). Ambiguous NOEs and automated NOE assignment. *Prog. NMR Spectrosc.* 32, 107–139.
- Pascal, S., Muhandiram, D.R., Yamazaki, T., Forman-Kay, J.D., and Kay, L.E. (1994). Simultaneous acquisition of ¹⁵N and ¹³C edited NOE spectra of proteins dissolved in H₂O. *J. Magn. Reson. B.* 103, 197–201.
- Pelton, J.G., Torchia, D.A., Meadow, N.D., and Roseman, S. (1993). Tautomeric states of the active-site histidines of phosphorylated and unphosphorylated III^{Glc}, a signal-transducing protein from *Escherichia coli*, using two-dimensional heteronuclear NMR techniques. *Protein Sci.* 2, 543–558.
- Pires, J.R., Parthier, C., Aido-Machado, R., Wiedemann, U., Otte, L., Bohm, G., Rudolph, R., and Oschkinat, H. (2005). Structural basis for APPTPLPP peptide recognition by the FBP11WW1 domain. *J. Mol. Biol.* 348, 399–408.
- Pires, J.R., Taha-Nejad, F., Toepert, F., Ast, T., Hoffmuller, U., Schneider-Mergener, J., Kuhne, R., Macias, M.J., and Oschkinat, H. (2001). Solution structures of the YAP65 WW domain and the variant L30 K in complex with the peptides GTPPPYTVG, N-(n-octyl)-GPPPY and PLPPY and the application of peptide libraries reveal a minimal binding epitope. *J. Mol. Biol.* 314, 1147–1156.
- Rotin, D., Staub, O., and Haguener-Tsapis, R. (2000). Ubiquitination and endocytosis of plasma membrane proteins: role of Nedd4/Rsp5p family of ubiquitin-protein ligases. *J. Membr. Biol.* 176, 1–17.
- Sakata, T., Sakaguchi, H., Tsuda, L., Higashitani, A., Aigaki, T., Matsuno, K., and Hayashi, S. (2004). *Drosophila* Nedd4 regulates endocytosis of notch and suppresses its ligand-independent activation. *Curr. Biol.* 14, 2228–2236.
- Sattler, M., Schleucher, J., and Griesinger, C. (1999). Heteronuclear multidimensional NMR experiments for the structure determination of proteins in solution employing pulsed field gradients. *Prog. NMR Spectrosc.* 34, 93–158.
- Schild, L., Lu, Y., Gautschi, I., Schneeberger, E., Lifton, R.P., and Rossier, B.C. (1996). Identification of a PY motif in the epithelial Na⁺ channel subunits as a target sequence for mutations causing channel activation found in Liddle syndrome. *EMBO J.* 15, 2381–2387.
- Schultz, J., Milpetz, F., Bork, P., and Ponting, C.P. (1998). SMART, a simple modular architecture research tool: identification of signaling domains. *Proc. Natl. Acad. Sci. USA* 95, 5857–5864.
- Seavey, B.R., Farr, E.A., Westler, W.M., and Markley, J.L. (1991). A relational database for sequence-specific protein NMR data. *J. Biomol. NMR* 1, 217–236.
- Snyder, P.M., Price, M.P., McDonald, F.J., Adams, C.M., Volk, K.A., Zeiher, B.G., Stokes, J.B., and Welsh, M.J. (1995). Mechanism by which Liddle's syndrome mutations increase activity of a human epithelial Na⁺ channel. *Cell* 83, 969–978.
- Snyder, P.M., Olson, D.R., McDonald, F.J., and Bucher, D.B. (2001). Multiple WW domains, but not the C2 domain, are required for inhibition of the epithelial Na⁺ channel by human Nedd4. *J. Biol. Chem.* 276, 28321–28326.
- Staub, O., Dho, S., Henry, P., Correa, J., Ishikawa, T., McGlade, J., and Rotin, D. (1996). WW domains of Nedd4 bind to the proline-rich PY motifs in the epithelial Na⁺ channel deleted in Liddle's syndrome. *EMBO J.* 15, 2371–2380.
- Tear, G., Harris, R., Sutaria, S., Kilomanski, K., Goodman, C.S., and Seeger, M.A. (1996). Commissureless controls growth cone guidance across the CNS midline in *Drosophila* and encodes a novel membrane protein. *Neuron* 16, 501–514.
- Toepert, F., Knaute, T., Guffler, S., Pires, J.R., Matzdorf, T., Oschkinat, H., and Schneider-Mergener, J. (2003). Combining SPOT synthesis and native peptide ligation to create large arrays of WW protein domains. *Angew. Chem. Int. Ed. Engl.* 42, 1136–1140.

- Verdecia, M.A., Bowman, M.E., Lu, K.P., Hunter, T., and Noel, J.P. (2000). Structural basis for phosphoserine-proline recognition by group IV WW domains. *Nat. Struct. Biol.* 7, 639–643.
- Viguera, A.R., Arrondo, J.L., Musacchio, A., Saraste, M., and Serano, L. (1994). Characterization of the interaction of natural proline-rich peptides with five different SH3 domains. *Biochemistry (Mosc.)* 33, 10925–10933.
- Wiesner, S., Stier, G., Sattler, M., and Macias, M.J. (2002). Solution structure and ligand recognition of the WW domain pair of the yeast splicing factor Prp40. *J. Mol. Biol.* 324, 807–822.
- Wilkin, M.B., Carbery, A.M., Fostier, M., Aslam, H., Mazaleyrat, S.L., Higgs, J., Myat, A., Evans, D.A., Cornell, M., and Baron, M. (2004). Regulation of Notch endosomal sorting and signaling by *Drosophila* Nedd4 family proteins. *Curr. Biol.* 14, 2237–2244.
- Wolf, B., Seeger, M.A., and Chiba, A. (1998). Commissureless endocytosis is correlated with initiation of neuromuscular synaptogenesis. *Development* 125, 3853–3863.
- Yamazaki, T., Forman-Kay, J.D., and Kay, L.E. (1993). Two-dimensional NMR experiments for correlating $^{13}\text{C}\beta$ and $^{13}\text{C}\alpha/\text{E}$ chemical shifts of aromatic residues in ^{13}C -labeled proteins via scalar couplings. *J. Am. Chem. Soc.* 115, 11054–11055.
- Yu, H., Chen, J.K., Feng, S., Dalgarno, D.C., Brauer, A.W., and Schreiber, S.L. (1994). Structural basis for the binding of proline-rich peptides to SH3 domains. *Cell* 76, 933–945.
- Zarrinpar, A., and Lim, W.A. (2000). Converging on proline: the mechanism of WW domain peptide recognition. *Nat. Struct. Biol.* 7, 611–613.
- Zwahlen, C., Legault, P., Vincent, S., Greenblatt, J., Konrat, R., and Kay, L.E. (1997). Methods for measurement of intermolecular NOEs by multinuclear NMR spectroscopy: application to a bacteriophage lambda N-peptide/box B RNA complex. *J. Am. Chem. Soc.* 119, 6711–6721.

Accession Numbers

NMR resonance assignments for the dNedd4 WW3*-Comm LPSY peptide complex have been deposited in the BioMagResBank (Seavey et al., 1991) with the accession code 6890. Coordinates and NMR-derived restraints have been deposited in the Protein Data Bank with the accession code 2EZ5.